Seismic fragility curves for limited ductile RC Buildings including the response of gravity frames

Anita Amirsardari[1*], Helen M. Goldsworthy[2*], Elisa Lumantarna[3*], Pathmanathan Rajeev[4]

1. Corresponding Author. PhD Candidate, Department of Infrastructure Engineering, University of Melbourne, Parkville, 3010, Australia.
   Email: amia@student.unimelb.edu.au

2. Associate Professor, Department of Infrastructure Engineering, University of Melbourne, Parkville, 3010, Australia. Email: helenmg@unimelb.edu.au

3. Lecturer, Department of Infrastructure Engineering, University of Melbourne, Parkville, 3010, Australia. Email: elu@unimelb.edu.au

4. Senior Lecturer, Department of Civil and Construction Engineering, Swinburne University of Technology, Hawthorn, 3122, Australia. Email: prajeev@swin.edu.au

[*] Bushfire and Natural Hazards Cooperative Research Centre

Abstract

The aim of this study is to assess the seismic performance of limited ductile reinforced concrete buildings in line with performance-based earthquake engineering principles. Limited ductile RC buildings are vulnerable to undesirable and sudden brittle failures which need to be considered in nonlinear models. The response of both the primary lateral load resisting system and the gravity load resisting system is considered. A brief description of the modelling approaches adopted to simulate the response of the core walls and frame components in a macro-finite element modelling space is provided. Using the adopted approach the seismic performance of two generic buildings with a symmetric plan is assessed. Nonlinear time-history analyses are conducted to obtain the building response to seismic ground motion. Probabilistic seismic demand model is developed using 'Cloud' analysis. Finally, fragility curves are developed considering four different performance limits to assess the seismic risk of the buildings.

Keywords: Limited ductile reinforced concrete, moment resisting frames, seismic assessment, fragility curves, cloud analysis

1 INTRODUCTION

This study is part of an on-going research project which aims to assess the seismic performance of vulnerable RC buildings in Australia by following performance-based earthquake engineering (PBEE) principles. PBEE aims to improve the design and assessment methods used to determine the buildings' behaviour under seismic loading in order to improve seismic risk mitigation decisions (Deierlein et al., 2003). Performance-based seismic assessment specifically aims to quantify the likely response of buildings to different intensities of seismic excitation via a probabilistic approach. The performance-based seismic assessment procedure can be summarised in to four key stages: (i) defining the likely characteristics of ground motions occurring at the site of interest and selecting suitable ground motion intensity measures (IM) to represent the level of earthquake shaking and hence the associated return periods, (ii) conducting nonlinear computer simulations to determine the building response to seismic ground motions by evaluating suitable engineering demand parameters (EDP) to develop the probabilistic seismic demand model (PSDM), (iii) developing fragility curves which define the probability of exceeding a certain performance limit for a given ground motion intensity, and (iv) relating the probability of performance limits being reached to losses in terms of costs for repair and retrofitting of buildings, downtime and casualties.

This study describes the procedure followed to develop fragility curves for RC buildings designed in Australia in the 1980s, and therefore it involves quantifying the first three stages of the performance-based seismic assessment procedure. Careful consideration has been given to creating the nonlinear models of the RC buildings in a macro-finite element modelling space. The buildings assessed have been designed with building components classified as *ordinary* detailing in accordance with the Concrete Structures Standard (Standards Australia, 1988). Hence, the buildings assessed have limited and/or non-ductile detailing with building components that are vulnerable to undesirable and sudden failures which are not necessarily captured using standard modelling techniques. Therefore, it is necessary to investigate the most suitable method to model the likely failure mechanisms of the various building components since damage limits of components are used to assess the structural performance limits of the building. Furthermore, the study involves an investigation of the performance of both the primary and secondary structural systems. This is because there are concerns about the performance of the gravity load resisting systems and the intensity of earthquake that may cause total collapse of a building. This is especially a concern in buildings with plan asymmetry which is to be investigated by the authors in the future studies. The current study presents the results for two RC buildings with plan symmetry. Time-history analyses are conducted to obtain the building response to various ground motion intensities. Cloud analysis is then used to develop the PSDM which is used to develop fragility curves for four performance limits.

2 BUILDING CHARACTERISTICS & EXPECTED COMPONENT RESPONSE

The seismic performance of a 5- and 9-storey RC building is assessed. These buildings have been designed in accordance with the concrete structures standard, AS 3600 (Standards Australia, 1988) and guidance from experienced structural engineers in Australia. The buildings consist of core walls which form part of the primary lateral-load resisting system and have therefore been designed to resist 100 % of the lateral loads due to wind. The walls have not been designed to resist seismic loads since seismic design was not mandated on a national basis until 1995 when the requirement for earthquake loading and design was referred to in the Building Code of Australia. The gravity load resisting system of the buildings constructed in the 1980s typically included perimeter frames with deep beams (600-900 mm deep) to satisfy fire requirements, and band-beams or flat-slab floor systems with column spacing of 7.0 to 8.4 m. Hence, the perimeter frames have significantly higher stiffness than the interior gravity system and therefore they will be subjected to greater seismic forces in comparison to the interior gravity system. Therefore, only the perimeter frames are modelled for the purpose of assessment of the gravity system. Summary of the key design details of the building component design is provided in Table 1, and the plan drawings of the buildings are provided in Figure 1. The box core walls represent stairwells and the C-shaped cores represent the lift shaft, the dimensions of the cores are provided in Table 2.

Table 1: Summary of design properties for building components

	Slab	**Edge beams**	**Columns**	**Core walls**
f'_c **(MPa)**	25	25	40	40
f_y **(MPa)**	400	400	400	400
ρ_l **(%)**	0.67-1.33	1.30-2.70	2.0-4.0	0.23-0.24
ρ_t **(%)**	0.25	0.23	0.075-0.12	0.25

f'_c: characteristic concrete compressive strength | f_y : nominal reinforcement yield strength | ρ_l: longitudinal reinforcement ratio | ρ_t: transverse reinforcement ratio

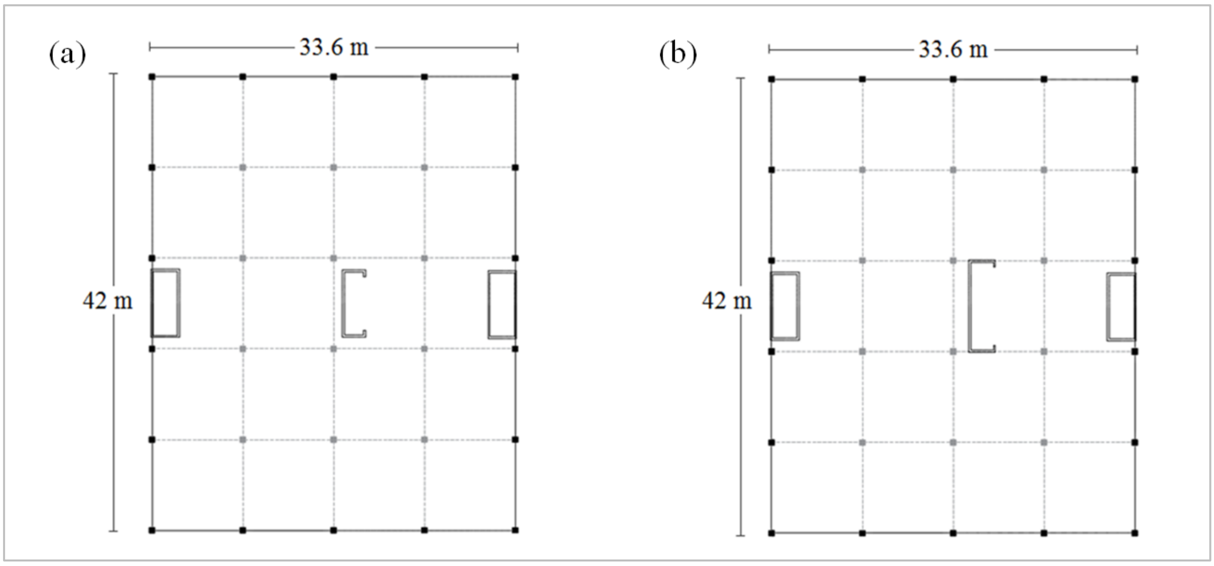

Figure 1: Building plan for: (a) 5-storey building, and (b) 9-storey building

Table 2: Core wall dimensions (in mm)

	Web length	Flange length	Return length	Wall thickness
Box core*	6300	2650	-	200
5-storey C-shaped core	6200	2200	600	200
9-storey C-shaped core	8500	2500	600	200

* Box core dimensions are the same for the 5- and 9-storey building

The walls that are assessed are lightly reinforced (i.e. they have low longitudinal reinforcement ratios) and have cracking moment capacities greater than the yield moment capacities. Therefore the walls are likely to develop a single crack (or minimal cracking) at the base since the area of reinforcing steel is insufficient to develop the tension forces required to form secondary cracks. Consequently, the walls are vulnerable to strain localisations and rupture of longitudinal bars (Henry, 2013; Hoult et al., 2017; Hoult, 2017).

The perimeter frames are designed as ordinary moment resisting frames (OMRFs) and have detailing deficiencies which are characteristic of limited ductile or non-ductile RC frames including: inadequate transverse reinforcement in beams and columns for shear strength and confinement, poor anchorage and splices of longitudinal bars in beams and columns (in particular bottom beam bars are terminated within the beam-column joint region with a short embedment length and splices of longitudinal bars located in potential hinge regions), columns having bending moment capacities which are approximately the same or less than the adjoining beams thus making the frame vulnerable to the undesirable weak-column strong-beam scenario under lateral loading, and inadequate transverse reinforcement in beam-column joint regions. Based on these detailing deficiencies and observations from previous earthquakes, it is essential that the nonlinear failure mechanisms of the columns and beam-columns joints are modelled accurately as they are likely to fail first and to cause global collapse of the building (Ghannoum & Moehle, 2012; Park & Mosalam, 2013).

3 FINITE ELEMENT MODELLING OF RC BUILDING

Nonlinear models of the buildings are created in the finite element analysis package, OpenSEES (McKenna et al., 2000). The columns, beams, and walls are modelled using concentrated plasticity elements since they ensure numerical efficiency and reliability for global analysis.

The nonlinear response of the column and beam are defined with a four point backbone curve to define the moment rotation material model. The four critical points represent cracking, nominally yield, ultimate capacity and deformation at shear failure, and axial load failure (which corresponds to approximately when lateral strength is equal to zero). The moment capacities are obtained by conducting moment-curvature analysis of the columns and the beams under gravity load for earthquake conditions in accordance with AS 1170.0 (Standards Australia, 2002). The rotational limits for the columns (and beams) are calculated based on the deformations experienced by a double curvature column. The deformation limit at nominal yield includes flexural, bar-slip, and shear displacements. The deformation limits at shear failure and axial load failure are calculated based on the drift limits proposed by Elwood and Moehle (2003) for flexure-shear critical columns. It is noted that the critical parameter which defines the drift at axial load failure of the columns is the axial load ratio. Experimental tests conducted in Australia on columns with detailing typically defined as ordinary or lightly reinforced columns have demonstrated to have significant drift capacity beyond ultimate strength if the axial load ratio is low and in contrast, columns with the same detailing have illustrated very limited drift capacity if heavily loaded axially (Fardipour, 2012; Wibowo et al., 2014; Wilson et al., 2015). The details and validation of the drift limits at shear and axial load failure has been discussed in Amirsardari et al. (2016). Furthermore, the comparison between the simulated response and experimental results available in the literature for two flexure-shear critical columns under medium and high axial load ratios are illustrated in Figure 2 (a) and (b).

Beam-column joint response is modelled using the scissor’s model approach with rigid links. A four point backbone is used to define the shear stress-strain response which is then converted to a moment-rotation response using the joint and frame dimensions as suggested by Celik and Ellingwood (2008). The critical shear stress points represent cracking (first point), shear induced in the joint due to the columns or beams reaching yield (second point) and ultimate bending capacity (third point), and the residual strength of the joint which is taken as 20 % of the maximum joint shear stress (fourth point). In the case of the second and third points the maximum shear is limited to the shear strength of the joint which is calculated using a strut and tie modelling approach. The shear strains corresponding to the critical shear stress values are based on the recommendations by Jeon et al. (2015). Furthermore, bar-slip of bottom beam reinforcement bars is considered by reducing the beam bending capacity under positive moment as suggested by Celik and Ellingwood (2008). The comparison between the simulated results using the proposed approach and the experimental results for an exterior joint subassemblage is provided in Figure 2 (c).

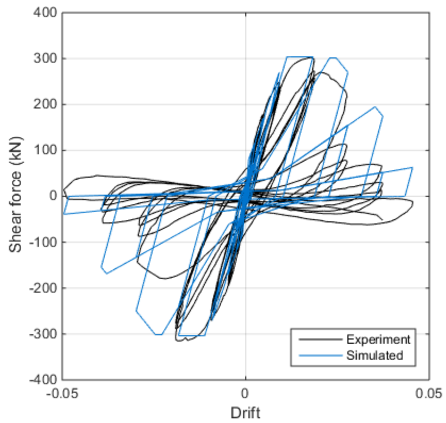

(a) Comparison between simulated and experimental results for flexure-shear critical column tested by Sezen (2002) with axial load ratio of 15 %

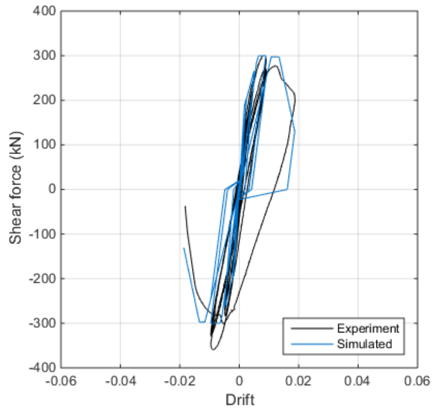

(b) Comparison between simulated and experimental results for flexure-shear critical column tested by Sezen (2002) with axial load ratio of 60 %

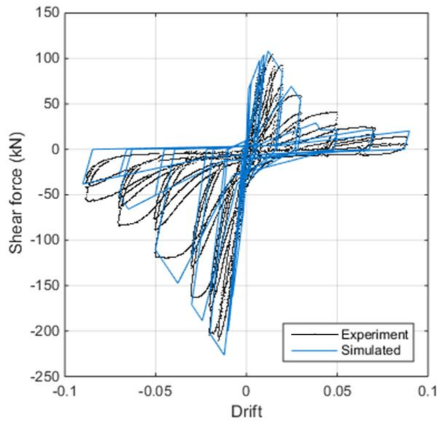

(c) Comparison between simulated and experimental results for a joint subassemblage tested by Pantelides et al. (2002) which failed in shear and slip of poorly anchored bottom beam bars

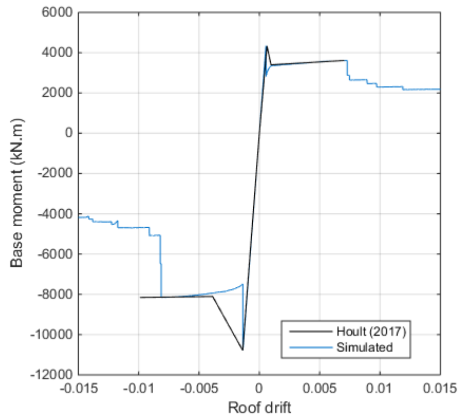

(d) Comparison between simulated pushover curve for 5-storey C-shaped core and predicted backbone response by Hoult (2017)

Figure 2: Validation of adopted component modelling methods

The walls are modelled with a single moment-rotation spring at the base of each core wall since it is expected that the walls will form a single crack at the base. The backbone response of the core walls is obtained by first conducting a pushover analysis of each core wall using distributed plasticity force-based elements. A single force-based element with two integration points is modelled at the base of the wall with a length equal to twice the plastic hinge length; the remaining portion of the wall is modelled with force-based elements with five integration points. The exclusive modelling of the plastic hinge region is necessary to ensure that the distribution of plasticity is representative of the true wall response and it also provides a method for calibrating and improving the strain predictions obtained from nonlinear analysis using distributed plasticity elements (Scott & Fenves, 2006). This is critical for the assessment of the walls since their response is determined via strain limits. The adopted plastic hinge length is based on the findings of Hoult et al. (2017) and Hoult (2017), which has also been validated by comparison with limited experimental results available for lightly reinforced rectangular walls. Furthermore, the response obtained for the C-shaped cores using the method described provides similar deformation limits as the equations provided by Hoult (2017) which have been developed based on extensive local finite element modelling of lightly reinforced C-shaped walls. The comparison between the simulated pushover results and the deformation limits predicted by Hoult (2017) for the five-storey C-shaped wall is provided in Figure 2 (d).

The hysteretic behaviour of the components is based on recommendations and calibrations with experimental results. Rayleigh damping is used with tangent stiffness proportional damping constant calibrated to provide 5 % equivalent viscous damping ratio for the first elastic mode. Furthermore, the expected mean material properties have been adopted based on Australian based studies and manufacturer's specifications.

4 PERFORMANCE LIMITS

There are many different performance limits which are defined in the literature and codes, each with different acceptance criteria. Table 3 summarises the limits adopted in this study, and Figure 3 provides a graphical representations of the limits for the various building components. Separate performance limits are defined for the primary and secondary structural systems, a similar approach is recommended by ASCE/SEI 41 (2013). Furthermore, where appropriate, drift limits are also provided to control the damage caused to non-structural components.

Table 3: Summary of the proposed performance limits

Performance limit	Primary structure (Walls)	Secondary structure (Frames)	Non-structural drift limit
Serviceability (S)	Wall reaching cracking rotational limit	Frame component reaching nominal yield rotational limit	0.004
Damage Control (DC)	Wall reaching a compressive strain of 0.002, or tensile strain of 0.015, whichever occurs first	Frame component reaching rotation which is at mid-point between yield and ultimate rotational limits	0.008
Life Safety (LS)	Wall reaching ultimate rotational limit, corresponding to a compressive strain of 0.004, or tensile strain of $0.6\varepsilon_{su}$, whichever occurs first	Frame component reaching the rotation corresponding to shear failure	0.015
Collapse Prevention (CP)	NA	Frame component reaching the rotation corresponding to 50 % reduction in ultimate lateral strength	NA

NA: Not applicable

The strain limits recommended for the walls are predominantly based on the detailed reasoning presented in Priestley et al. (2007) for the *Serviceability* and *Damage Control* performance limit. However, the recommendations by Priestley et al. (2007) generally relate to the response of ductile components, therefore, the strain limits are reduced in this study such that they are representative of the level of damage expected for limited ductile components. The drift limits adopted are also typically lower than recommendations by other studies, guidelines, and codes for the higher performance limits (i.e. *Life Safety* and *Collapse*

Prevention) (FEMA 2003; Standards New Zealand, 2004; Sullivan et al., 2012) due to the lack of consideration given to the seismic drift capacity of non-structural components in older buildings (and new buildings) (McBean, 2008).

Furthermore, in this study significant effort has been made to define the axial load failure of frame elements which form part of the gravity load resisting system. This is because there are concerns about the axial load capacity of the gravity system and the ability of this system to deform together with the lateral load resisting system, as well as the response of this system after the lateral load resisting system loses its lateral stiffness. Therefore, the *Collapse Prevention* performance limit is based on the axial failure limit reached by the perimeter frame components. It is also noted that in this study it is assumed that the frame elements will undergo axial load failure prior to the primary lateral load resisting system. This is because the walls take relatively low axial load and it is expected that they will be able to sustain this load even under displacements that occur after the ultimate lateral strength capacity is reached.

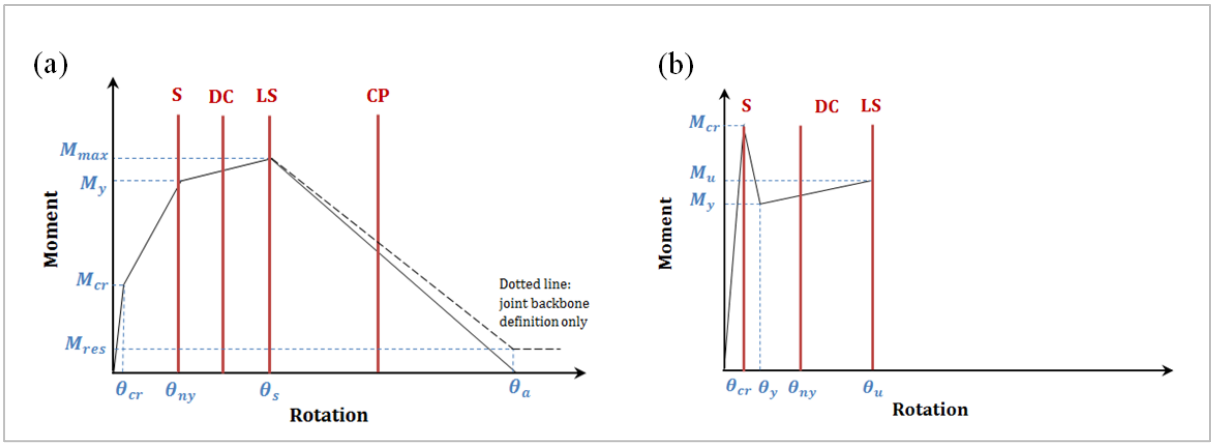

Figure 3: Graphical representation of performance limits: (a) frame components, (b) walls

5 FRAGILITY CURVES

Seismic fragility curves define the probability of exceeding a damage limit state as a function of ground motion intensity measure (IM). It is most commonly defined via the lognormal cumulative distribution function. The damage limit state may be defined using a single or multiple engineering demand parameters (EDPs). In this study, the performance limits for the buildings are based on when the first component in a building reaches a structural damage limit or when the interstorey drift demand exceeds the non-structural drift limits. Therefore, the EDP adopted is the critical demand-to-capacity ratio (ϒ) which corresponds to the component response or interstorey drift that will first cause the building to reach the performance limit (Jalayer et al., 2007). The analytical fragility curve can be computed using Eq. 1.

$$P[\Upsilon > 1|IM] = \phi \frac{\ln(\eta_{\Upsilon|IM})}{\sqrt{\beta_{\Upsilon|IM}^2 + \beta_C^2 + \beta_M^2}} \qquad \text{Eq. 1}$$

Where ϕ is the standard normal cumulative distribution function
$\eta_{\Upsilon|IM}$ is the median critical demand-to-capacity ratio as a function IM
$\beta_{\Upsilon|IM}$ is the dispersion (logarithmic standard deviation) of the critical demand-to-capacity ratio as a function of IM

β_C is the dispersion of the structural capacity uncertainty
β_M is the dispersion of the modelling uncertainty

5.1 PROBABILISTIC SEISMIC DEMAND MODEL

To compute the fragility curve it is necessary to first develop a probabilistic seismic demand model (PSDM) which relates the EDP to the intensity measure. There are various procedures used to obtain the PSDM; the well-established methods which are obtained through conducting dynamic nonlinear time history analysis (THA) are incremental dynamic analysis (IDA), multiple stripe analysis (MSA), and cloud analysis.

IDA and MSA both involve conducting multiple time history analyses at incrementally increasing IM and therefore both methods have the capability to produce the most complete PSDM, however, this also makes them computationally very expensive. Furthermore, both methods usually involve the use of scaled records which may cause loss of true earthquake characteristics especially when large scaling factors are used.

The most efficient method of obtaining the PSDM is by conducting cloud analysis. It involves using unscaled records to obtain a *cloud* of intensity-response data points. Regression analysis is conducted for the cloud of data to approximate the PSDM parameters. The method requires significantly less THA since multiple analyses at a certain IM is not necessary. However, record selection plays a key role on the accuracy of the method and it is recommended that the suite of records selected cover a wide range of IM and that a significant portion of the records provide data points near the damage limit state (i.e. for this study when $\Upsilon = 1$) (Jalayer et al., 2017; Rajeev et al., 2014). Furthermore, unscaled records must be used which eliminates the issues related to using scaled records. Another key advantage of the cloud analysis method is that for the same set of analyses different IMs may be selected to obtain different PSDM and from the regression analyses it is possible to select the best IM to represent the demand quantity (Rajeev et al., 2008; Rajeev et al., 2014). A disadvantage of cloud analysis is that it assumes a constant conditional standard deviation for the probability distribution of the engineering demand parameter given IM (Jalayer et al., 2014). The method was in fact initially utilised by Cornell et al. (2002) to support a power-law demand model with a constant standard deviation of the natural logarithm, provided in Eq. 2. More complex demand models have been proposed by other researchers (Aslani & Miranda, 2005) however, studies have illustrated that Eq. 2 is capable of providing accurate results and it is preferred due to its simplicity and because it ensures closed-form solutions (Rajeev et al., 2014).

$$D_{50\%} = a.IM^b \quad \text{Eq. 2}$$

Where $D_{50\%}$ is the conditional median demand parameter
a *and* b are the parameters obtained from regression analysis

In this study the cloud analysis method is adopted to obtain the PSDM due the advantages discussed above. Furthermore, Eq. 2 is adopted to approximate the fragility function parameters.

5.2 GROUND MOTIONS

Forty-five unscaled records have been selected to conduct dynamic time-history analyses. The records have been selected such that they cover a wide range of IM values and are characteristic of Australian earthquakes. The records selected are a combination of: (i) stochastically generated records obtained using the program *GENQKE* (Lam, 1999) which is capable of producing ground motions that are representative of Australian earthquakes, (ii) historical records with characteristics representative of Australian earthquakes, including that they are shallow earthquakes with reverse fault mechanisms (Brown & Gibson, 2004), (iii) simulated records on soil conditions by using the non-linear site response program *DEEPSOIL* (Hashash et al., 2016) and using generated and historical rock records as input ground motions.

6 RESULTS & DISCUSSION

PSDMs are obtained for the 5- and 9-storey RC buildings by conducting dynamic time-history analyses by applying the ground motions along the weaker axes of the buildings. Statistically, the most suitable IM to develop the fragility curves is the IM which provides the highest correlation with the PSDM and hence the lowest dispersion ($\beta_{Y|IM}$). Therefore, regression analysis is conducted for the PSDMs using different IMs to obtain the dispersion for each performance limit. The IMs investigated are: peak ground acceleration (PGA), peak ground velocity (PGV), peak ground displacement (PGD), maximum spectral acceleration response (RSA_{max}), maximum spectral displacement response (RSD_{max}), the spectral acceleration and displacement response at the fundamental building period (T_1) and at multiples of the fundamental building period ($1.5T_1$ and $2.0T_1$). The dispersion obtained for the various IMs are displayed in Figure 4 and Figure 5 for the 5- and 9-storey building, respectively. It can be seen that the PGD, RSD_{max}, $RSA(2T_1)$ and $RSD(2T_1)$ provide the lowest dispersion for the four different performance limits for both buildings.

In addition to selecting an IM that provides a high correlation between the IM and EDP, it is also important to select an IM which is capable of accurately representing ground motion intensities that can be related to earthquake return periods. Spectral response parameters dependant on the fundamental period are highly sensitive to the spectral shape and are therefore difficult to relate to existing design response spectra. In addition, there are uncertainties associated with determining the building fundamental period. Therefore, based on the statistical results and the reliability and familiarity of RSD_{max}, it has been chosen as the IM to be used to assess the performance of the RC buildings analysed in this study.

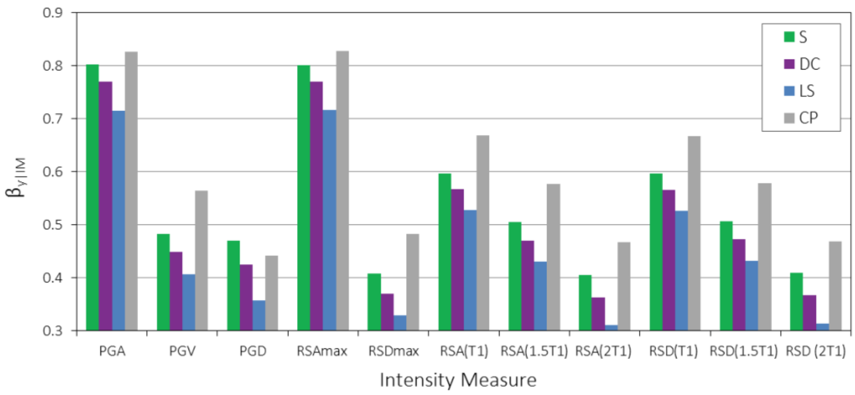

Figure 4: Dispersion factors for 5-storey building

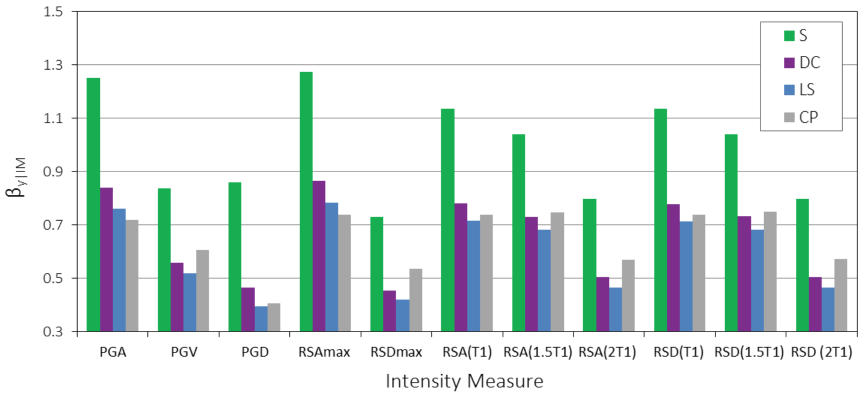

Figure 5: Dispersion factors for 9-storey building

The PSDMs for the four performance limits for the 5- and 9-storey buildings are shown in Figure 6 and Figure 7, respectively. The fragility curves for both buildings are presented in Figure 8. It is noted that in this study the dispersion due to capacity and modelling uncertainty has not been considered. To provide an indication of the associated earthquake return period events, the corresponding RSD_{max} is calculated for a 500 and 2500 year return period (YPR) event in accordance with AS 1170.4 (Standards Australia, 2007) for a city with a hazard factor (Z) of 0.1 g. A range of RSD_{max} exists for each return period since it has been calculated for the five site classes in AS 1170.4:2007, ranging from hard-rock to very soft soil sites. The results show that under a 500 YRP event it is very likely that the 5- and 9-storey buildings will reach and exceed the *Serviceability* and *Damage Control* limit. Furthermore, the results in general show that both buildings are highly likely to reach the *Life Safety* limit state if they are located on soil sites under a 2500 YRP event. However, they have a low probability of reaching the *Collapse Prevention* limit under a 2500 YRP event.

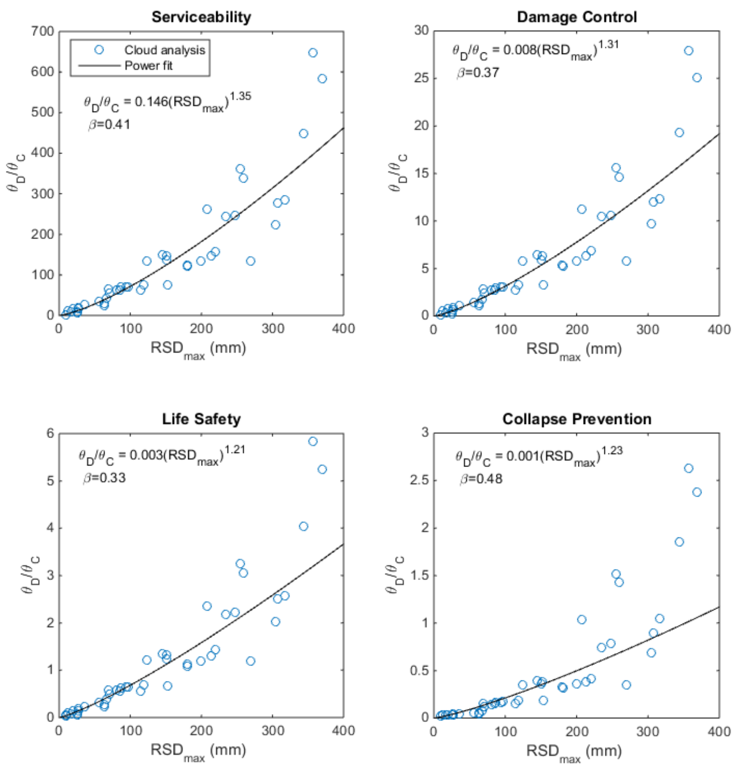

Figure 6: PSDM using cloud analysis for the 5-storey building

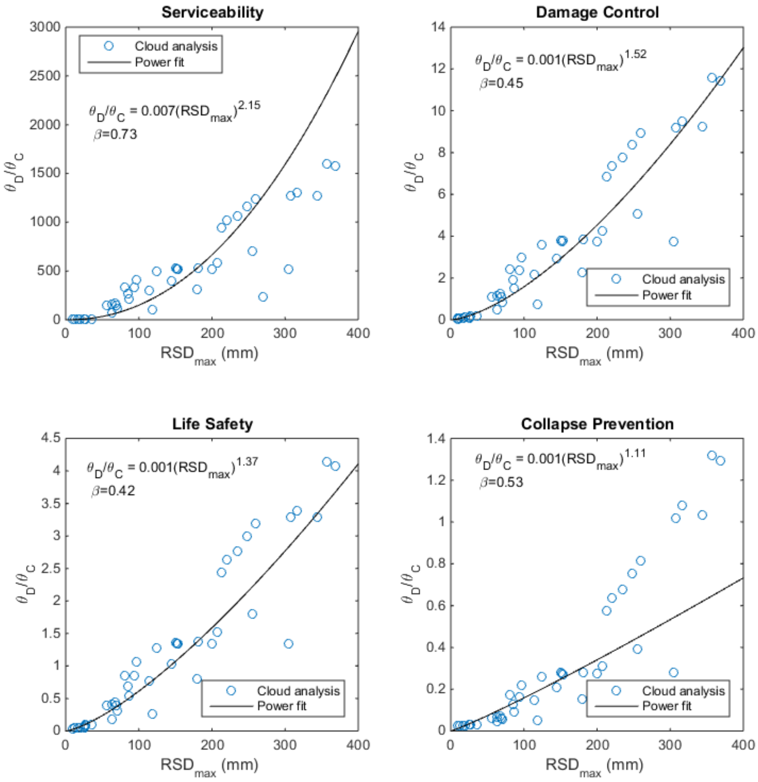

Figure 7: PSDM using cloud analysis for the 9-storey building

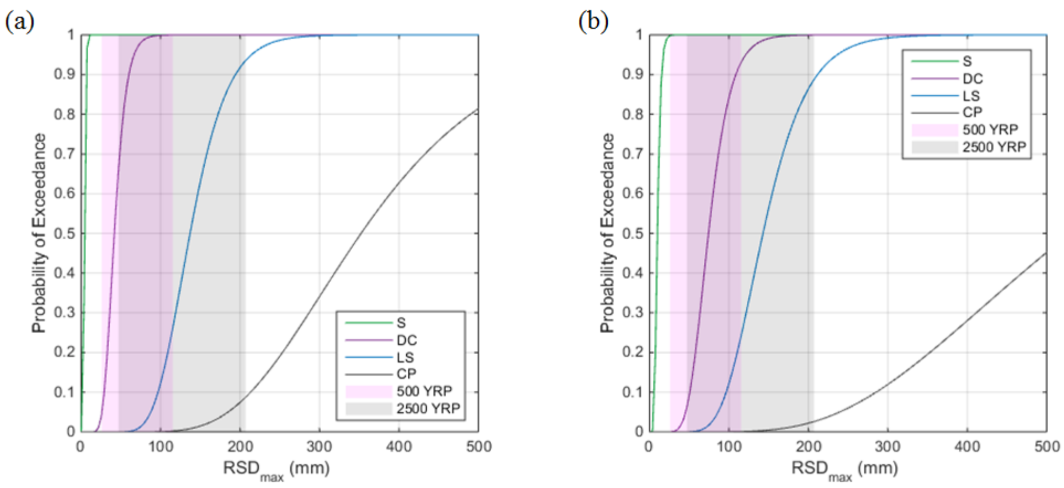

Figure 8: Fragility curves with RSD_{max} as IM: (a) 5-storey building, and (b) 9-storey building

7 CONCLUSION

This study has described the procedure followed to conduct performance-based seismic assessments for limited ductile RC buildings. Fragility curves are presented for two generic RC buildings (5- and 9-storey) which are symmetrical in plan and with characteristics of buildings constructed in Australia in the 1980s. The response for both the primary and secondary structural system is assessed by conducting dynamic time-history analyses in order to develop fragility curves. The probabilistic seismic demand model is obtained by using cloud analysis as it is the most computational efficient method and hence suitable when assessing the global response of non-linear buildings modelled in 3D. In addition, the method allows for the same set of analyses to select different IMs to develop the PSDM, this provided the opportunity to illustrate the importance in carefully selecting IM for developing fragility curves.

The results from the analyses show that under a 500 YRP event it is very likely that the 5- and 9-storey buildings will reach and exceed the *Damage Control* limit. In addition, it is also observed that under a 2500 YRP event it is likely that both buildings will reach the *Life Safety* limit, however, they have a low probability of reaching the *Collapse Prevention* limit as defined in this study.

8 REFERENCE LIST

American Society of Civil Engineers (ASCE/SEI). (2013). Seismic evaluation and retrofit of existing buildings. Reston, Virginia: American Society of Civil Engineers.

Amirsardari, A., Rajeev, P., Goldsworthy, H. M., & Lumantarna, E. (2016). *Modelling non-ductile reinforced concrete columns.* Paper presented at the Australian Earthquake Engineering Society 2016 Conference, Melbourne, Victoria.

Aslani, H., & Miranda, E. (2005). Probability-based seismic response analysis. *Engineering Structures, 27*(8), 1151-1163. doi: 10.1016/j.engstruct.2005.02.015

Brown, A., & Gibson, G. (2004). A multi-tiered earthquake hazard model for Australia. *Tectonophysics, 390*(1-4), 25-43. doi: 10.1016/j.tecto.2004.03.019

Celik, O. C., & Ellingwood, B. R. (2008). Modeling Beam-Column Joints in Fragility Assessment of Gravity Load Designed Reinforced Concrete Frames. *Journal of Earthquake Engineering, 12*(3), 357-381. doi: 10.1080/13632460701457215

Cornell, C. A., Jalayer, F., Hamburger, R. O., & Foutch, D. A. (2002). Probabilistic basis for 2000 SAC Federal Emergency Management Agency steel moment frame guidelines. *Journal of Structural Engineering, 128*(8), 526-533. doi: 10.1061//ASCE/0733-9445/2002/128:4/526

Deierlein, G. C., Krawinkler, H., & Cornell, C. A. (2003). *A framework for performance-based earthquake engineering*. Paper presented at the 2003 Pacific Conference on Earthquake Engineering.

Elwood, K. J., & Moehle, J. P. (2003). Shake table tests and analytical studies on the gravity load collapse of reinforced concrete frames *Pacific Earthquake Engineering Research Center, PEER Report 2003/01*. University of California, Berkeley.

Fardipour, M. (2012). *Seismic performace of limited-ductile RC columns in moderate seismicity regions.* (PhD thesis), Department of Infrastructure Engineering, The University of Melbourne.

Federal Emergency Management Agency (FEMA). (2003). Multi-hazard loss estimation methodology, earthquake model: HAZUS MR4 Technical Manual. Washington, D.C.: Federal Emergency Management Agency.

Ghannoum, W. M., & Moehle, J. P. (2012). Rotation-Based Shear Failure Model for Lightly Confined RC Columns. *Journal of Structural Engineering, 138*(10), 1267-1278. doi: 10.1061/(asce)st.1943-541x.0000555

Hashash, Y. M. A., Musgrove, M. I., Harmon, J. A., Groholski, D. R., Phillips, C. A., & Park, D. (2016). DEEPSOIL 6.1. Retrieved from http://deepsoil.cee.illinois.edu/

Henry, R. S. (2013). *Assessment of the minimum vertical reinforcement limits for RC walls.* Paper presented at the New Zealand Society Earthquake Engineering (NZSEE) Conference, Auckland, New Zealand.

Hoult, R., Goldsworthy, H., & Lumantarna, E. (2017). Plastic hinge length for lightly reinforced rectangular concrete walls. *Journal of Earthquake Engineering*. doi: 10.1080/13632469.2017.1286619

Hoult, R. D. (2017). *Seismic assessment of reinforced concrete walls in Australia.* (PhD Thesis), Department of Infrastructure Engineering, The University of Melbourne, Melbourne, Australia.

Jalayer, F., De Risi, R., & Manfredi, G. (2014). Bayesian Cloud Analysis: efficient structural fragility assessment using linear regression. *Bulletin of Earthquake Engineering, 13*(4), 1183-1203. doi: 10.1007/s10518-014-9692-z

Jalayer, F., Ebrahimian, H., Miano, A., Manfredi, G., & Sezen, H. (2017). Analytical fragility assessment using unscaled ground motion records. *Earthquake Engineering & Structural Dynamics*. doi: 10.1002/eqe.2922

Jalayer, F., Franchin, P., & Pinto, P. E. (2007). A scalar damage measure for seismic reliability analysis of RC frames. *Earthquake Engineering & Structural Dynamics, 36*(13), 2059-2079. doi: 10.1002/eqe.704

Jeon, J.-S., Lowes, L. N., DesRoches, R., & Brilakis, I. (2015). Fragility curves for non-ductile reinforced concrete frames that exhibit different component response mechanisms. *Engineering Structures, 85*, 127-143. doi: 10.1016/j.engstruct.2014.12.009

Lam, N. T. K. (1999). "GENQKE" User's Guide: Program for generating synthetic earthquake accelerograms based on stochastic simulations of seismological models. Department of Civil and Environmental Engineering, The University of Melbourne, Australia.

McBean, P. C. (2008). Drift intolerant facade systems and flexible shear walls: Do we have a problem. *Australian Journal of Structural Engineering, 8*(1), 77-84.

McKenna, F., Fenves, G. L., Scott, M. N., & Jeremic, B. (2000). Open System for Earthquake Engineering Simulation (OpenSEES) (Version 2.4.5, 2013): Pacific Earthquake Engineering Research Center, University of California, Berkeley, CA. Retrieved from http://opensees.berkeley.edu/

Pantelides, C. P., Hansen, J., Nadauld, H., & Reaveley, L. D. (2002). Assessment of reinforce concrete building exterior joints with substandard details *PEER 2002/18*: Pacific Earthquake Engineering Center, University of California, Berkeley.

Park, S., & Mosalam, K. M. (2013). Simulation of reinforced concrete frames with nonductile beam-column joints. *Earthquake Spectra, 29*(1), 233-257. doi: 10.1193/1.4000100

Priestley, M. J. N., Calvi, G. M., & Kowalsky, M. J. (2007). *Displacement-based seismic design of structures*. Pavia, Italy: IUSS Press.

Rajeev, P., Franchin, P., & Pinto, P. E. (2008). Increased accuracy of vector-IM-based seismic risk assessment? *Journal of Earthquake Engineering, 12*(sup1), 111-124. doi: 10.1080/13632460801925798

Rajeev, P., Franchin, P., & Tesfamariam, S. (2014). *Probabilistic seismic demand model for RC frame buildings using cloud analysis and incremental dynamic analysis.* Paper presented at the Tenth U.S. National Conference on Earthquake Engineering (NCEE), Anchorage, Alaska.

Scott, M. H., & Fenves, G. L. (2006). Plastic hinge integration methods for force-based beam-column elements. *Journal of Structural Engineering, 132*(2), 244-252. doi: 10.1061//ASCE/0733-9445/2006/132:2/244

Sezen, H. (2002). *Seismic behavior and modeling of reinforced concrete columns.* (PhD Dissertation), University of California, Berkeley.

Standards Australia. (1988). AS 3600-1988: Concrete structures.

Standards Australia. (2002). AS 1170.4-2002: Structural design actions, Part 0: General principles. Sydney, NSW.

Standards New Zealand. (2004). NZS 1170.5:2004 Structural design actions - Part 5: earthquake actions - New Zealand. Wellington.

Sullivan, T. J., Priestley, M. J. N., & Calvi, G. M. (2012). *A model code for the displacement-based seismic design of structures*. Instituto Universitario di Studi Superiori di Pavia: IUSS Press.

Wibowo, A., Wilson, J. L., Lam, N. T. K., & Gad, E. F. (2014). Drift performance of lightly reinforced concrete columns. *Engineering Structures, 59,* 522-535. doi: 10.1016/j.engstruct.2013.11.016

Wilson, J. L., Wibowo, A., Lam, N. T. K., & Gad, E. F. (2015). Drift behaviour of lightly reinforced concrete columns and structural walls for seismic design applications. *Australian Journal of Structural Engineering, 16*(1). doi: 10.7158/s14-002.2015.16.1